ISSN: 2978-7270

Journal of Oil, Petroleum and Natural Gas Research

Review Article

Open Access

Geodynamics and Seismicity of the Anatolian-Caucasian-Arabian Region and the Earthquakes in Turkey on February 6, 2023 and on April 23, 2025

Svalova Valentina

Sergeev Institute of Environmental Geoscience, Russian Academy of Sciences, 13 building 2 Ulansky per, Moscow 101000, Russian Federation, Geophysical Institute, Vladikavkaz Scientific Center, Russian Academy of Sciences,93a Markova Str, Vladikavkaz 362002, Russian Federation

ABSTRACT

A magnitude 7.8 earthquake occurred in southeastern Turkey on February 6, 2023. The earthquake's location is associated with the triple junction of the Anatolian, Arabian, and African plates and is confined to the East Anatolian Fault, which forms the boundary between the Anatolian and Arabian plates.

The North Anatolian Fault separates the Eurasian and Anatolian tectonic plates, which slide relative to each other at a rate of 2 cm per year. Earthquakes occur regularly along this fault, and activity is gradually shifting further west, into the Sea of Marmara, toward Istanbul. The segment of this zone adjacent to the city has not been active for 250 years. The development of geodynamic models of the deep structure of disaster-prone areas is an important contribution to the study of active continental margins, which is necessary for earthquake prevention, prediction, and forecasting, geoecological risk assessment, and disaster preparedness.

The geodynamic model of the Anatolian-Caucasian-Arabian region is determined by mantle flow rising from the core surface and propagating beneath the lithosphere, creating complex surface velocities in Anatolia to the west, in the Arabian Plate to the east, and in the Caucasus to the north. This flow will continue to transport material along the North Anatolian and East Anatolian Faults.

The frequency of strong earthquakes varies along the faults, due to the varying crustal thickness and rheology of the fault environment. The Moho depth of the East Anatolian Fault is approximately 40 km, while that of the North Anatolian Fault is approximately 50 km. Along the North Anatolian Fault, strong earthquakes occur every 1-10 years (1939, 1942, 1943, 1944, 1953, 1957, 1966, 1967, 1971, 1992, 1999) with hypocenters spaced approximately 100 km apart and pointing west. Since the 1999 Izmit earthquake occurred 80 km east of Istanbul, an earthquake in the Istanbul area can be expected within a few years (1-10 years).

Because the East Anatolian Fault produced strong earthquakes in 1789 (M 7.2), 1795 (M 7.0), 1872 (M 7.2), 1874 (M 7.1), 1875 (M 6.7), 1893 (M 7.1), 2020 (M 6.8), and 2023 (M 7.8, M 7.7), therefore, the recurrence interval of these groups (1790–1880–2020) is approximately 100 years. However, within these groups, there are typically 2–4 strong earthquakes occurring close in time. It can be predicted that a strong earthquake on the East Anatolian Fault, if not occurring within 1–2 years after 2023, will occur only in 100 years.

***Corresponding author**

Svalova Valentina, Sergeev Institute of Environmental Geoscience, Russian Academy of Sciences, 13 building 2 Ulansky per, Moscow 101000, Russian Federation, Geophysical Institute, Vladikavkaz Scientific Center, Russian Academy of Sciences,93a Markova Str, Vladikavkaz 362002, Russian Federation.

Received: March 03, 2026; **Accepted:** March 09, 2026; **Published:** March 17, 2026

Keywords: Earthquake, Geodynamics, Lithosphere, Caucasus, Turkey, Modeling

Introduction

After every huge natural catastrophe the question of prognosis, forecast, reasons and monitoring arises. New systems of monitoring and scientific and emergency organizations will be suggested in the countries. New approaches to the problem of the earthquakes prognosis and prediction must be elaborated. The results of event must be analyzed at the new scientific level on the base of new geological-geophysical data. Huge victims demand new efforts for the problems decision -long-term, medium-term and short- term forecasts of disasters and earthquake resistant construction. One of important steps could be elaboration of geodynamic model of the region of catastrophic event as basis for all possible geological-geophysical data collection and analysis at different scale with aim of future forecast, prediction and prognosis.

2023 Turkey-Syria Earthquake

Earthquake of M 7.8 struck south -eastern Turkey and north -western Syria on 6 February 2023, at 04:17 of local time. The epicenter was 37 km west–northwest of Gaziantep. The earthquake hypocenter was at a depth of 10.0 km according to USGS. The earthquake was followed by a M 7.7 earthquake at 13:24. This earthquake was centered 95 km north-northeast from the first.

The M 7.8 earthquake is the largest in Turkey since the 1939 Erzincan earthquake of the same magnitude, and the second-strongest recorded in the country, after the 1668 North Anatolia earthquake. It is also one of the strongest earthquakes ever recorded in the Levant. There were more than 10,000 aftershocks in the three weeks that followed. The seismic sequence was the result of shallow strike-slip faulting.

There was widespread damage in an area of about 350,000 km. An estimated 14 million people (16 percent of Turkey's population) were affected. About 1.5 million people were left homeless. More than 52,800 deaths were confirmed: more than 46,100 in Turkey, and more than 6,700 in Syria. It is the deadliest earthquake in Turkey since the 526 Antioch earthquake; deadliest in Syria since the 1822 Aleppo earthquake; deadliest worldwide since the 2010 Haiti earthquake; and the fifth-deadliest of the 21st century. It is the deadliest natural disaster in Turkey's modern history. The earthquakes caused over US$100 billion in damages (the fourth-costliest earthquakes).

The location of the earthquake is connected with a triple junction between the Anatolian, Arabian, and African plates (Figure 1, 2, 3, 4).

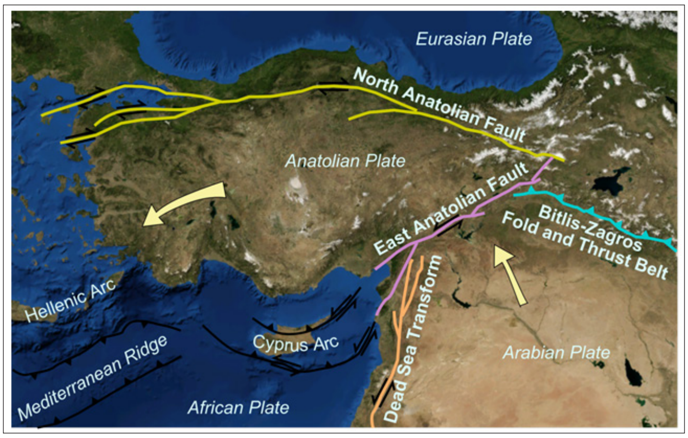

Figure 1: The Largest Systems of Active Faults in the Middle East: North Anatolian - Zagros and Levant - East Anatolian https://ru.wikipedia.org/wiki/Восточно-Анатолийский_разлом#/media/Файл:Anatolian_Plate.png

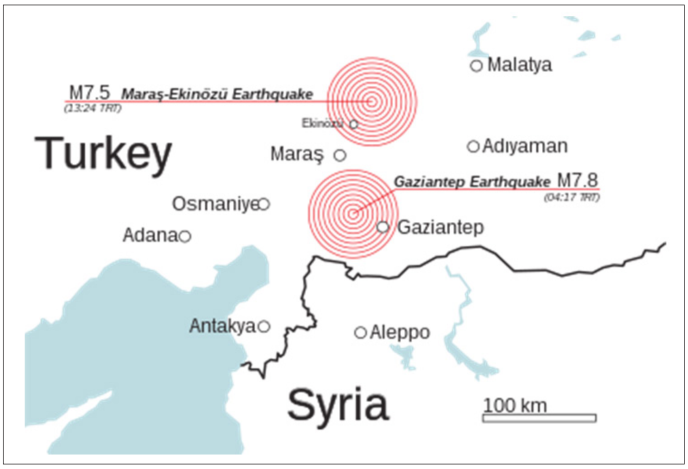

Figure 2: Epicenter Locations of the First and Second Major Earthquakes
https://en.wikipedia.org/wiki/File: 2023_Gaziantep-Marash_Earthquakes.svg

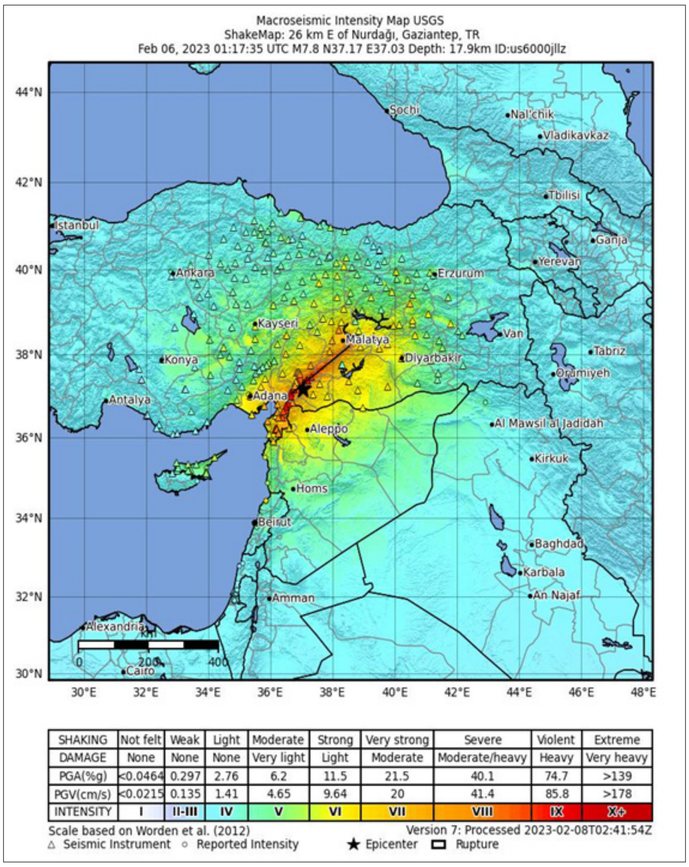

SHAKING	Not felt	Weak	Light	Moderate	Strong	Very strong	Severe	Violent	Extreme
DAMAGE	None	None	None	Very light	Light	Moderate	Moderate/heavy	Heavy	Very heavy
PGA(%g)	<0.0464	0.297	2.76	6.2	11.5	21.5	40.1	74.7	>139
PGV(cm/s)	<0.0215	0.135	1.41	4.65	9.64	20	41.4	85.8	>178
INTENSITY	I	II-III	IV	V	VI	VII	VIII	IX	X+

Figure 3: Distribution of the Intensity of an Earthquake of Magnitude 7.8 with an Epicenter Near the City of Gaziantep. Mw 7.8 Earthquake at 01:17 UTC (USGS)

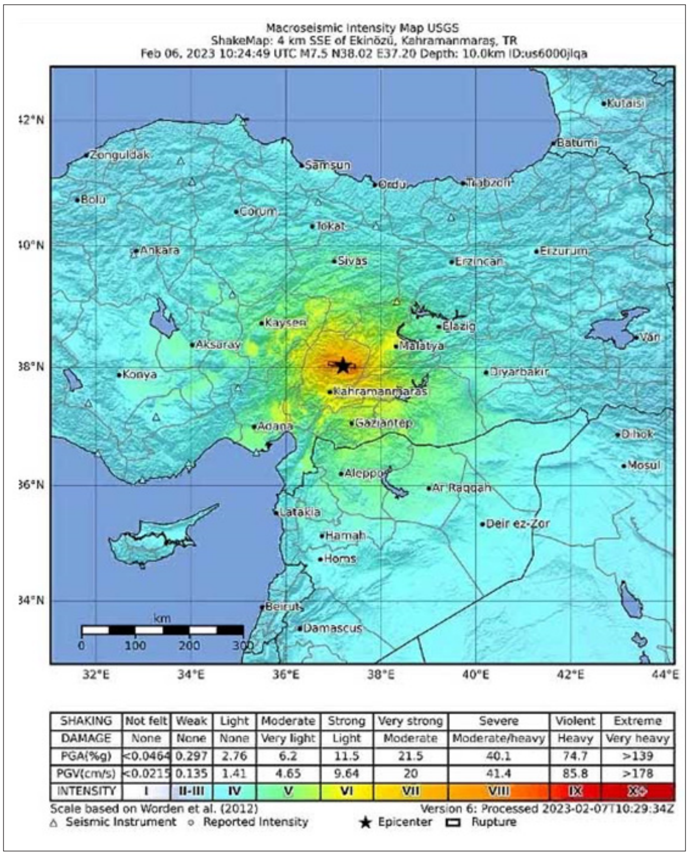

SHAKING	Not felt	Weak	Light	Moderate	Strong	Very strong	Severe	Violent	Extreme
DAMAGE	None	None	None	Very light	Light	Moderate	Moderate/heavy	Heavy	Very heavy
PGA(%g)	<0.0464	0.297	2.76	6.2	11.5	21.5	40.1	74.7	>139
PGV(cm/s)	<0.0215	0.135	1.41	4.65	9.64	20	41.4	85.8	>178
INTENSITY	I	II-III	IV	V	VI	VII	VIII	IX	X+

Figure 4: Strong Ground Motion Map. Kahramanmarash Earthquake. Mw 7.7 Earthquake at 10:24 UTC (USGS)

The East Anatolian Fault traces the westward movement of Turkey to the Aegean Sea. The Dead Sea Transform traces the northward motion of the Arabian Peninsula, relative to the Africa and Eurasia plates.

The East Anatolian Fault is a 700-kilometre-long northeast–southwest left-lateral transform fault and forms the boundary between the Anatolian and Arabian plates. This intracontinental transform fault is the second largest strike-slip fault in Turkey.

The fault slip rates decrease from the east at 10 mm per year to the west of 1–4 mm per year. The fault produced large earthquakes in 1789 (M 7.2), 1795 (M 7.0), 1872 (M 7.2), 1874 (M 7.1), 1875 (M 6.7), 1893 (M 7.1), and 2020 (M 6.8). The region of the 6 February 2023 earthquakes is relatively quiet seismologically (Figure 5).

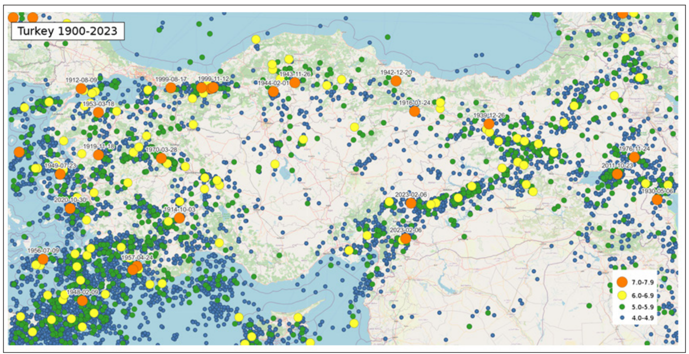

Figure 5: Map of Seismicity of Turkey (USGS)

It was waiting for strong earthquake in vicinity of Istanbul in connection with North Anatolian Fault, but not in connection with East Anatolian Fault. Geodynamic activity of the East Anatolian Fault is well investigated. (Figure 6-8).

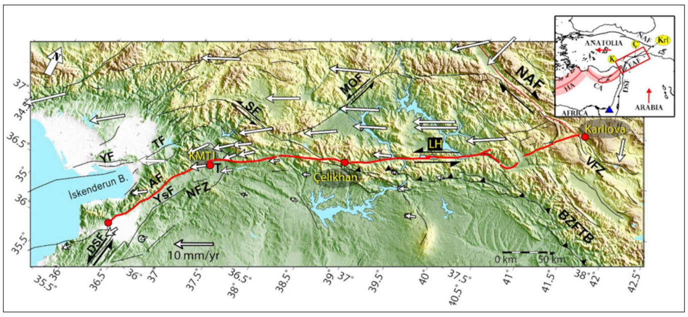

Figure 6: Tectonic Setting in the Region of the East Anatolian Fault (indicated by a bright red line). The Black Arrows along the Axis indicate the Relative Motion of the Fault walls. The white Arrows Indicate the Speeds of Movement in a Fixed Frame of Reference, Determined using GPS (the length of the Arrows Indicates the Magnitude of the Speed) [1].

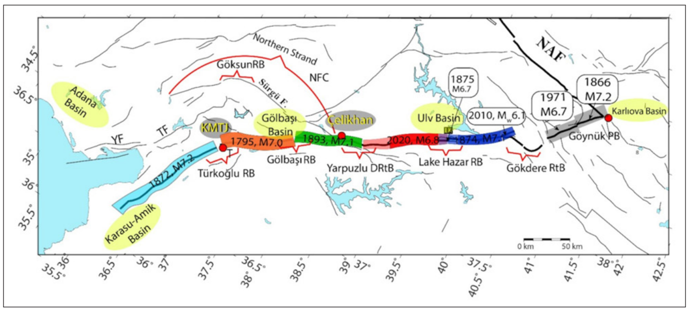

Figure 7: Sites on the East Anatolian Fault, Showing the Dates and Epicenters of the Largest Earthquakes Before the Event of February 6, 2023 [1].

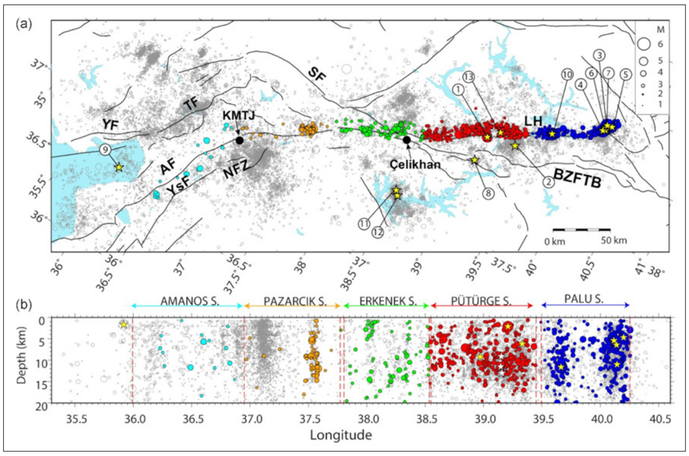

Figure 8: (a) Cartographic View and (b) Seismicity Depth Section along the East Anatolian Fault for the period 2007–2019. Earthquakes with a Magnitude Greater than 2.5 are Shown with Colored Circles According to the Segments. Seismicity was taken into Account Within 15 on Both Sides of the Fault Axis. Numbers Denote Events with a Magnitude Greater Than 5.0. KMTJ, Kahramanmarash Node; LH, Lake Khazar; BZFTB, Bitlis-Zagros belt; SF, Syorgyu fault; AF, Amanos fault; YsF, Esemek fault; YF, Yumurtalyk fault; TF, Toprakkale fault; NFZ - Narla Fault [1]. Only five earthquakes (1905, 1945, 1986, 1998) of magnitude 6.0 or larger have occurred there since 1905.

All these earthquakes occurred along or in the vicinity of the East Anatolian Fault. At the same time southern Turkey and northern Syria had significant and damaging earthquakes in the past. Aleppo, the second-largest city in Syria, was devastated several times historically by large earthquakes. Aleppo was struck by an estimated magnitude 7.1 earthquake in 1138 and an estimated magnitude 7.0 earthquake in 1822. Fatality estimates of the 1822 earthquake were 20,000–60,000. In 1114, the city of Marash suffered an earthquake which killed 40,000. Major earthquakes affecting the Middle East in 856, 1033 and 1754 have resulted in 200,000, 70,000 and 40,000 deaths, respectively.

Seismicity of the North Anatolian Fault Zone

On August 17, 1999, the devastating Izmit earthquake struck Turkey. Its magnitude was 7.7, the epicenter was at a depth of 17 km near the city of Izmit, 80 km east of Istanbul. According to official figures, the death toll was about 15,000 people, about 25,000 were injured, and 600,000 lost their homes. Damage from the earthquake was initially estimated at more than 25 billion dollars, but later increased by another 5-7 billion. The shocks were also felt in neighboring countries.

The North Anatolian Fault, the first largest strike-slip fault in Turkey, produced 11 large earthquakes during the 20th century (1939, 1942, 1943, 1944, 1953, 1957, 1966, 1967, 1971, 1992, 1999). (Figure 9).

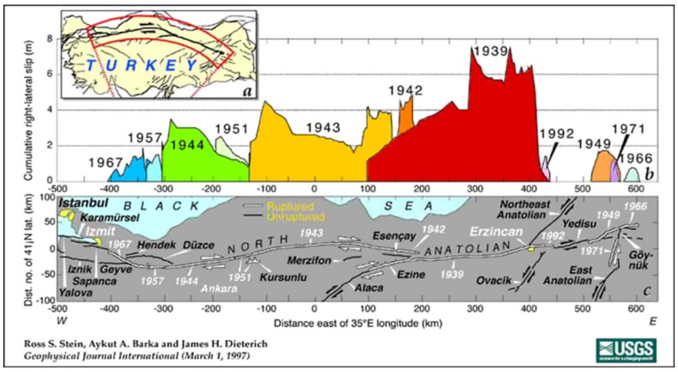

Figure 9 (a) Active Faults in Turkey, with the North Anatolian Fault in Bold. GPS Observations Establish a 24±4 mm/yr Deep Slip Rate on the North Anatolian Fault.

(b) Cumulative Right-lateral Slip Associated with M>=6.7 Earthquakes the Sequence Ruptured from Warm to Cool Colors. Slip in the 1949, 1966, and 1971 Shocks is Approximate

(c) The Region Inscribed by the Solid Red Line in a is Projected Relative to the Anatolia-Eurasia Rotation Pole, So that a Transform Fault would Strike Due East-West; the North Anatolian Fault is Seen to Deviate Less than 40 km from Being a Simple Right-Lateral Transform [2].

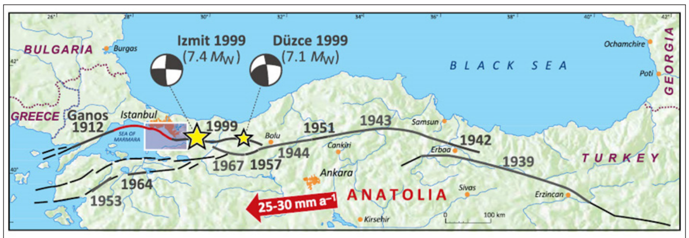

Figure 9 (d). North Anatolian Fault and Earthquakes of 1939-1999 [3].

Turkey is located in a seismically hazardous zone, its territory is crossed by the active North Anatolian Fault Zone (NAFZ), which separates the Eurasian and Anatolian tectonic plates, sliding relative to each other at a speed of 2 cm per year. Earthquakes constantly occur along it, and activity gradually shifts further and further west into the Sea of Marmara, towards Istanbul. The segment of this zone adjacent to the city has not been activated for 250 years, and this gives 2 options for the development of events. In the first case, there is a constant and low-amplitude sliding of the plates relative to each other and the tectonic stress is removed in the form of a "silent earthquake". In the second case the absence of slip means the accumulation of stress in the fault zone, which, when it reaches a critical value, can be released by a sharp shock of enormous force. And that spells imminent disaster for Istanbul, a city of 14 million people. This is why studying and monitoring the state of the NAFZ is truly vital for Turkey.

In 2014 work began on the project to create a Deep Geophysical Observatory on the North Anatolian Fault (GONAF) of the International Continental Scientific Drilling Program (ICDP). These studies are carried out jointly by Turkish and German scientists. To monitor the seismic state of the NAFZ in the land areas closest to the main branch of the fault, the islands of Yassyada and Sivriada of the Princes' Islands of the Sea of Marmara, seismic stations are installed in wells up to 500 m deep, constantly monitoring microshocks along the dangerous segment with high resolution. (Figure 10).

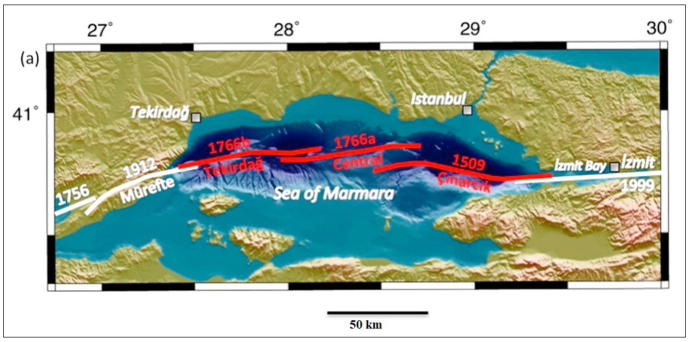

Figure 10: Red Line - the Sea of Marmara Segment, Inactive Since 1766
http://www.gonaf.de/content/project/index.html

Also an international group of scientists from France and Germany undertook to study the underwater part of the NAFZ segment, located a few dozen kilometers from Istanbul. For this, a network of 10 transponders was installed at the bottom of the Marmara Sea in October 2014. (Figure 11).

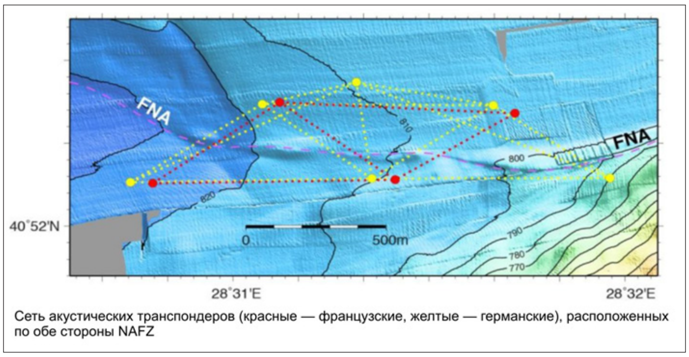

Figure 11: Network of Acoustic Transponders (Red - German, Yellow French), Located on Both Sides of the North Anatolian Fault
https://www.sciencedaily.com/releases/2016/07/160713115102.htm

The data obtained show that there are no significant movements along the fault within the resolution of the system. The distance between transponders located at a distance of 350 to 1,700 meters from each other is measured with a resolution of 1.5–2 mm. Based on the data obtained, scientists came to the preliminary conclusion that the segment is blocked or almost blocked and accumulates stress that can cause an earthquake. In combination with other types of monitoring, such work makes it possible to create a more complete and comprehensive picture of what is happening in this seismically hazardous region.

Earthquake in Turkey on April 23, 2025 and Seismicity of the Sea of Marmara

On April 23, 2025, at 12:49:10 local time (UTC+3:00), an earthquake with a magnitude of M 6.2 occurred in the Sea of Marmara. Its epicenter was located 21 km southeast of Marmara Ereglisi district, Tekirdag province, Turkey, 73 km southwest of Istanbul, with coordinates 40°49′58″ N 28°13′36″ E (Figure 12).

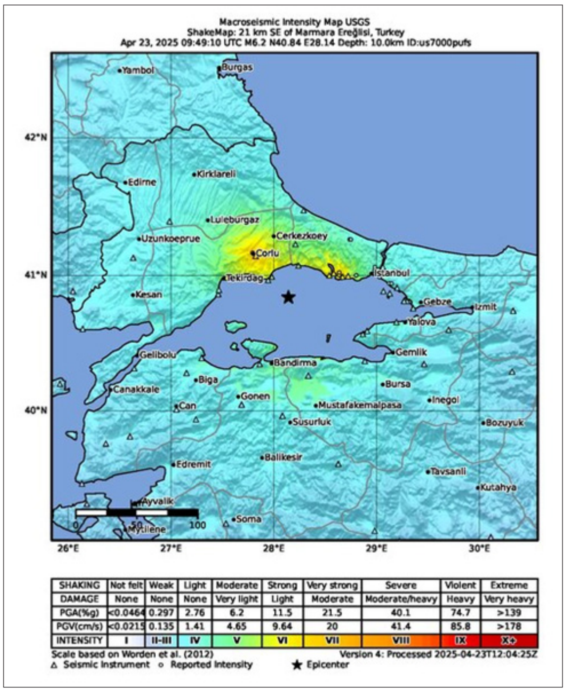

Figure 12: Epicenter of the Earthquake in the Marmara Sea on April 23, 2025 (USGS)

According to a report from Istanbul Technical University (ITU), the earthquake lasted 13 seconds and triggered 291 aftershocks. Plate displacement was only 30 cm—significantly less than the expected 3.7 meters. The aftershocks were distributed along a 40 x 12 km band, reaching depths of up to 30 km.

The maximum intensity rating on the modified Mercalli scale reached VII (very strong). According to various sources, the focal depth ranged from 10 to 16.9 km. The aftershocks were preceded by a magnitude 3.9 earthquake, which was recorded at 12:13 PM in the Sea of Marmara, near the town of Silivri.

It was followed by three more aftershocks, including a mainshock with a magnitude of 6.2. Two more earthquakes struck the Büyükçekmece region (41°01′12″N 28°34′39″E) within 11 minutes of each other. Their magnitudes were 4.4 and 4.9, respectively. According to the US Geological Survey, approximately 188,000 people were affected by intensity VII tremors. Intensity VI (strong) tremors were felt by approximately 2.28 million people, primarily in the western parts of Istanbul Province. Intensity IV (moderate) tremors were recorded in the central parts of Istanbul and Bursa, as well as in Evros (Greece), and in the cities of Burgas and Yambol (Bulgaria). Tremors were reported from as far away as Gaziantep, Bucharest (Romania), and Sofia (Bulgaria). At least 359 people were injured in the mass panic caused by jumping from heights, including 236 in Istanbul. An abandoned three-story building collapsed in the Fatih district. Damage to several buildings and internet outages were reported in parts of Istanbul. At least 3,597 rescue workers, including 1,443 in Istanbul, and 250 pieces of equipment were deployed in the Marmara region.

The city of Istanbul, with a population of approximately 16 million and once the capital of the Byzantine and Ottoman empires, is located dangerously close to the North Anatolian Fault, which runs 20 kilometers (12.4 miles) south of Istanbul across the Sea of Marmara. Each new strong earthquake provides additional information about seismicity in the region and allows for more accurate forecasting and prevention of future destructive events. The regular distribution of strong earthquakes along the North Anatolian Fault from east to west makes the Marmara earthquake a very important link in this chain and provides new data for the analysis of seismicity in the Istanbul region (Figure 13).

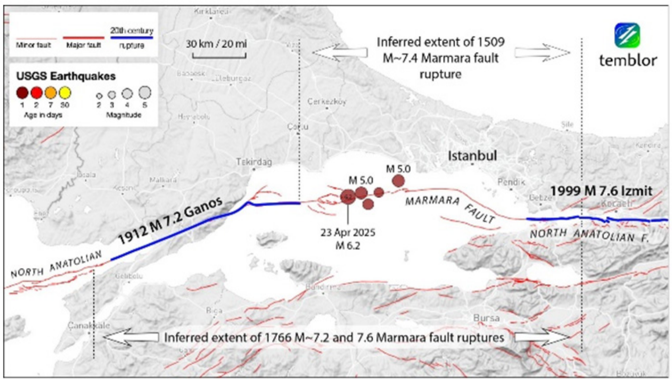

Figure 13: Earthquake in the Marmara Sea 23-4-2025 [4].

It is important to understand and examine how the 2025 Sea of Marmara earthquake compares to the large earthquakes along the North Anatolian Fault from 1939–1999, as well as to earlier historical earthquakes that caused significant damage to Istanbul and heavy casualties.

This requires a detailed analysis of the seismicity of the Sea of Marmara, as well as the deep geodynamics and geothermal environment of the entire Anatolian-Caucasian and surrounding regions. The major earthquakes in the Sea of Marmara region are presented in Table 1 and Figure 14.

Table 1: Earthquakes in the Sea of Marmara region from 1500–1999 with Magnitudes M≥ 6.0. The list is complete for Earthquakes with Magnitudes M≥ 6.8, but not for Weaker Events [5].

Year	Date	Time	Lat.	Long.	M
1509	9-10	2200	40.9	28.7	7.2
1556	5-10	2400	40.3	27.8	7.2
1719	5-25	1200	40.7	29.8	7.4
1737	3-6	0730	40.1	27.3	7.0
1754	9-2	0330	40.8	29.2	6.8
1766	5-22	0500	40.8	29.0	7.1
1766	8-5	0530	40.5	26.6	7.4
1809	2-7	0000	40.0	27.0	6.1
1826	2-8	2030	39.8	26.4	6.2
1841	10-6	0230	40.85	29.05	6.1
1850	4-19	2330	40.1	28.3	6.1
1855	2-28	0230	40.1	28.6	7.1
1855	4-11	1940	40.2	28.9	6.3
1859	8-21	1130	40.3	26.1	6.8
1860	8-22	1009	40.5	26.0	6.1
1893	2-9	1716	40.5	26.2	6.9
1894	7-10	1224	40.7	29.6	7.3
1912	8-9	0128	40.7	27.2	7.3
1912	8-10	0923	40.8	27.5	6.2
1912	9-13	2331	40.7	27.0	6.8
1935	1-4	1441	40.50	27.60	6.4

1935	1-4	1620	40.55	27.75	6.3
1943	6-20	1532	40.68	30.48	6.4
1944	10-6	0234	39.7	26.5	6.8
1953	3-18	1906	40.0	27.4	7.1
1956	2-20	2031	39.84	30.41	6.2
1957	5-26	0633	40.6	31.0	7.2
1963	9-18	1658	40.70	28.95	6.4
1964	10-6	1431	40.1	28.2	6.8
1967	7-22	1657	40.7	30.7	7.2
1975	3-27	0515	40.45	26.12	6.5
1983	7-5	1201	40.28	27.76	6.1
1999	8-17	0001	40.7	30.0	7.4

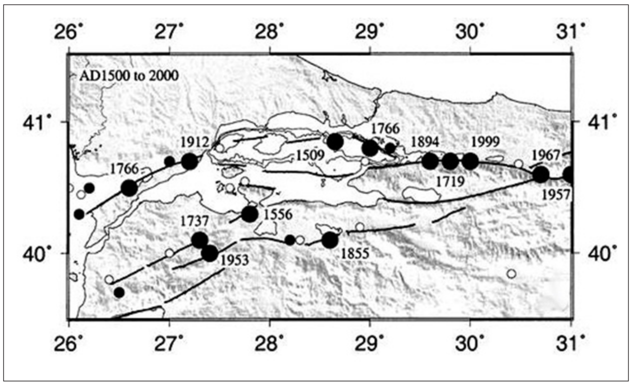

Figure 14: Earthquakes in the Sea of Marmara region During the Period 1500–1999 with magnitude M≥ 6.0. The Main Earthquakes in the Sea of Marmara Region are from Table 1. Large Black Circles are Events with M ≥ 7.0, Small Black Circles are those with 7.0 > M ≥ 6.6, and White Circles are those with 6.6 > M ≥ 6.0. Only those with M ≥ 7.0 are Labeled with Dates [5].

The historic Istanbul (Constantinople) earthquake occurred in the Bosphorus and Sea of Marmara region on September 10, 1509. The epicenter was located at 40°54′ N, 28°42′ E. The magnitude of the earthquake was 7.2 ± 0.3. Due to its severe consequences, it was nicknamed the Little Doomsday Earthquake (or the Doomsday Earthquake). Sultan Bayezid II was forced to move the capital to Edirne for several months. Estimates of the death toll range from 4,000 to 10,000.

The earthquake caused extensive damage to Istanbul (the Fatih Mosque, Topkapi Palace, and the Galata quarter) and the fortresses along the Bosphorus. The Princes' Islands were also damaged by the tremors and the resulting tsunami, which reached up to 6 meters in height. One of the most devastating earthquakes in the history of the Ottoman Empire occurred on May 22, 1766. Two strong aftershocks struck the Istanbul area. The first, with an estimated magnitude of 7.1 and an epicenter at 40°48′N 29°00′E / 40.8°N 29°E, occurred in the eastern part of the Sea of Marmara, in the Çınarcık Depression near the Princes' Islands. Between 4,000 and 5,000 people died. The two-minute earthquake destroyed numerous buildings. Aftershocks that followed the earthquake lasted for three months. The Fatih Mosque, built in 1463 by Sultan Mehmed II, known as Fatih (the Conqueror), was completely destroyed.

The strong historical earthquakes of 1509 and 1766 near Istanbul have led to the assumption that the recurrence period for strong earthquakes here is 250 years.

The North Anatolian Fault is a right-lateral strike-slip fault approximately 1,200 km long. It extends from the Gulf of Saros in the Aegean Sea in the west to the Karlovo Triple Fault at its junction with the East Anatolian Fault in the east. The fault began to form approximately 13-11 million years ago in eastern Anatolia and eventually spread westward. The fault in the Sea of Marmara region was fully formed approximately 200,000 years ago, although strike-slip movement in this zone began as early as the late Miocene.

In the eastern part of the North Anatolian Fault up to Izmit, the fault zone is a clearly defined morphological structure that follows the boundary between the Anatolian and Eurasian plates. The zone is fairly narrow and localized, effectively separating the relatively rigid regions of the Black Sea and Central Anatolia.

Right-lateral strike-slip faulting continues west of Izmit but becomes widespread in several subparallel belts in the Sea of Marmara, northwestern Turkey, and the northern Aegean [6,7]. Seismic studies in the Sea of Marmara reveal numerous faults with large normal components [Okay 1999], and earthquakes with normal fault mechanisms are observed around its margins [8]. The Sea of Marmara was presumably formed by pull-apart crustal extension. GPS studies indicate that east-west slip across the entire Figure 7 region is about 23 ± 3 mm/yr [9,10].

An important point is the transition of events to the Sea of Marmara region, which alters the rheological environment due to a decrease in crustal thickness and the dynamics of sedimentary basin formation and evolution. The observed seismicity patterns in the Sea of Marmara contribute to several earthquake prediction and warning issues. For example, it has been noted that the length of active elements of the North Anatolian Fault in the sea is shorter than onshore in the eastern part of the fault. Earthquakes in the sea are weaker than onshore. There are also seismic windows (gaps) where earthquakes have not occurred for many years. For example, the section of the North Anatolian Fault adjacent to Istanbul has not been active since 1766. A key point of the analysis is that the earthquake chain along the North Anatolian Fault, moving westward, skipped the city of Istanbul, which fits well with the concept of progradation, as the previous strong earthquake was the 1999 earthquake in the eastern Sea of Marmara. The 2025 earthquake has a lower magnitude of 6.2 compared to the magnitude of 7.6-7.7 in 1999, reflecting the transition to thinner marine crust with different rheology (Figure 15-17).

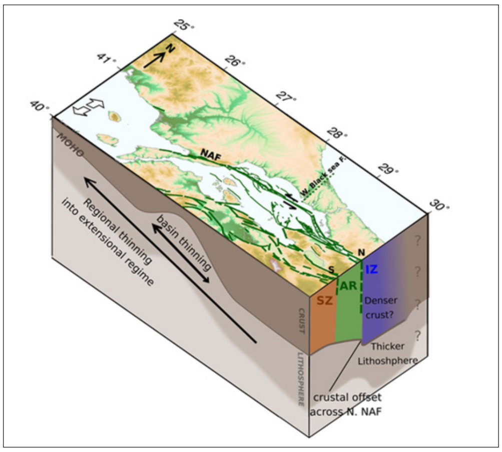

Figure 15: Crust Thinning in the Marmara Sea [11].

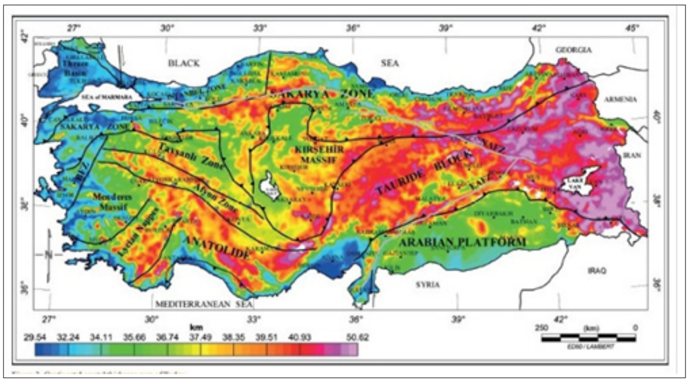

Figure 16: MOHO Boundary in Turkey [12].

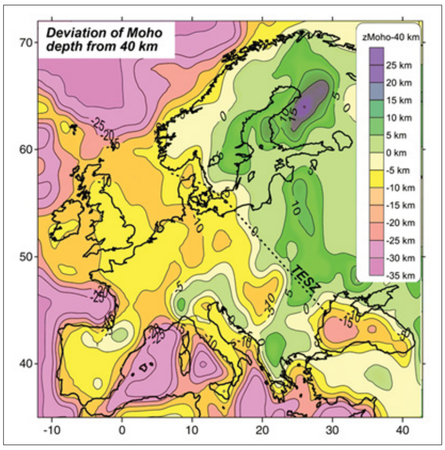

Figure 17: Structure of European Crust as Deviation of 40 km Thickness. TESZ – Trans European Sutur Zone [13].

If we assume that strong earthquakes propagating along the North Anatolian Fault from east to west have passed the Istanbul area and are moving further west toward the Aegean Sea, as evidenced by the 2025 earthquake west of Istanbul, this could indicate a decrease in seismic risk for Istanbul in the near future in terms of horizontal movements along the fault.

The historical 1509 and1766 earthquakes near Istanbul are not associated with a consistent westward movement of earthquakes along the fault, but reflect other important patterns. For example, it should be noted that seismicity in many sedimentary basins of the Alpine-Himalayan and Pacific belts is concentrated on the periphery of the basins, while the deepest parts of the depressions are characterized by reduced seismicity and increased heat flow (Figure 18-21). [14-16].

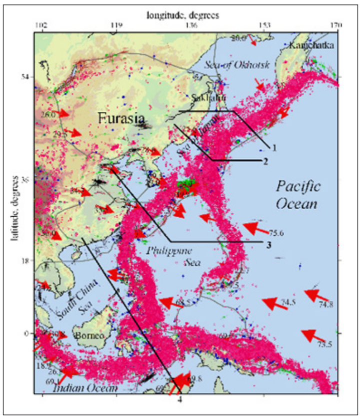

Figure 18: Seismicity of the Pacific Belt [17].

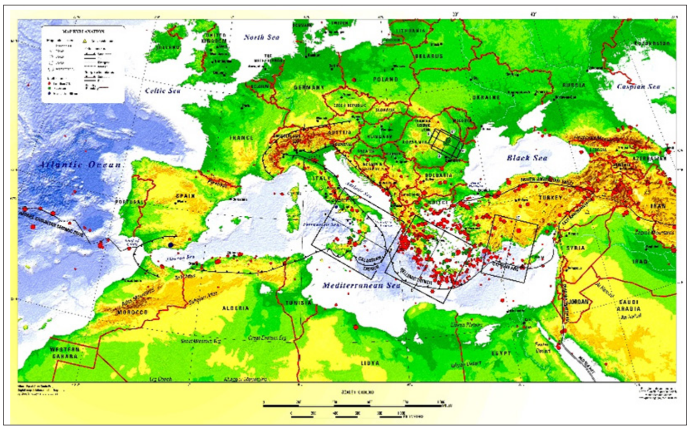

Figure 19: Seismicity of Mediterranean Sea and Surrounding Areas. (USGS)

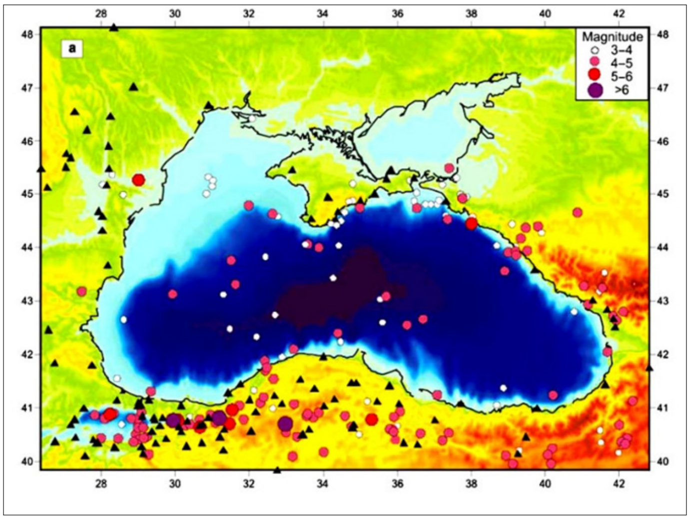

Figure 20: Seismicity of Black Sea (USGS)

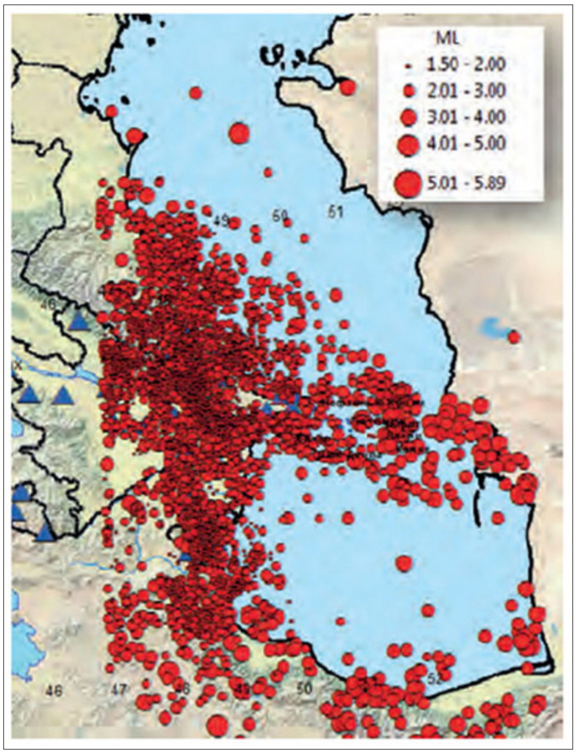

Figure 21: Seismicity of Caspian Sea (USGS)

These patterns are well explained by the upwelling of mantle diapirs during the formation of sedimentary basins. In the initial stages of basin formation, a domed uplift structure forms on the Earth's surface, followed by a deep depression, reflecting the geodynamics of diapir upwelling and cooling and the spreading of material above it due to gravitational instability [14,16]. A similar mechanism is evident in the Sea of Marmara. The upwelling of mantle masses thins the crust and increases heat flow beneath the basin. It is important to note that the entire Marmara Sea basin consists of individual depressions, which may reflect both the manifestation of gravitational instability in the form of the rise of individual diapirs, and the formation of the basin by the pull-apart mechanism of fault extension, when the rise of mantle matter in the center of the forming basins plays a passive role, filling the vacated space (Figure 22-24).

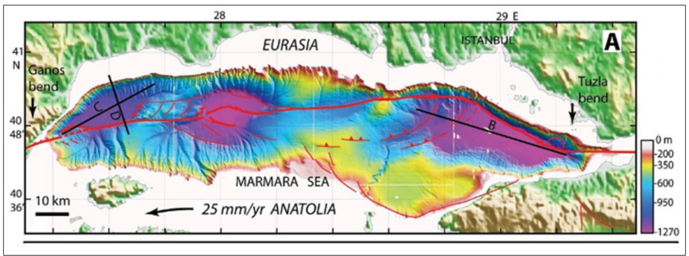

Figure 22: Bathymetry of Depressions of the Marmara Sea [18].

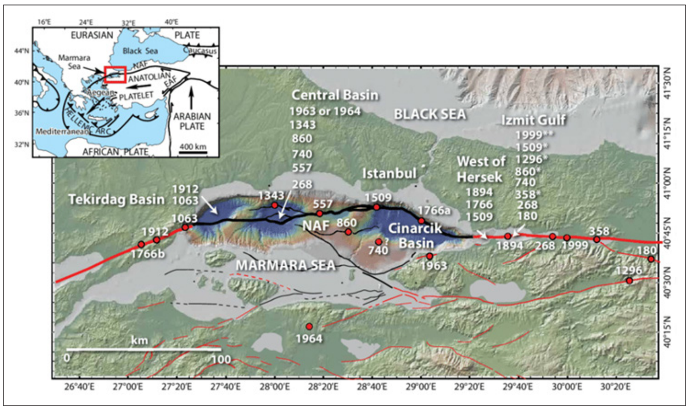

Figure 23: Historical Earthquakes of Marmara Sea [19].

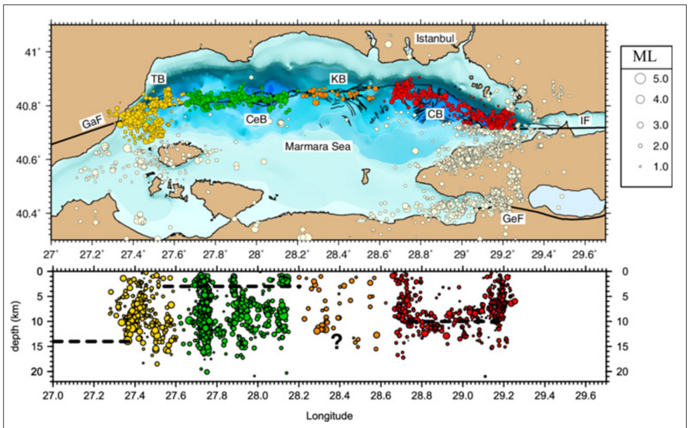

Figure 24: Map and Cross section of the Seismicity of Marmara Sea 2007-2012. The Tekirdag Basin (TB) in Yellow, the Central Basin (CeB) in Green, the Kumburgaz Basin (KB) in Orange, and the Cinarcik Basin (CB) in red. GaF for Ganos Fault, IF for Izmit Fault, and GeF for Gemlik Fault. Dotted lines in the Depth Section Show the Locking Depth of Each Domain [20].

Heat flow in the center of depressions is increased, and the depression boundaries are in a more brittle state, susceptible to earthquakes. The hotter environment in the center of depressions promotes lower viscosity and is less conducive to the accumulation of elastic stress energy for a subsequent earthquake, when the rock's ultimate strength is reached and stress release occurs (Figure 25-27).

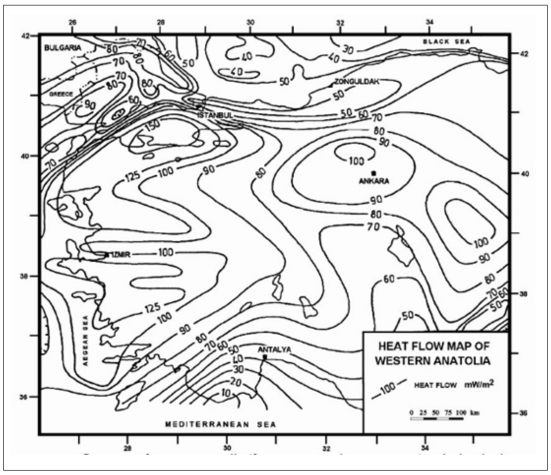

Figure 25: Heat Flow Map of Western Anatolia [21].

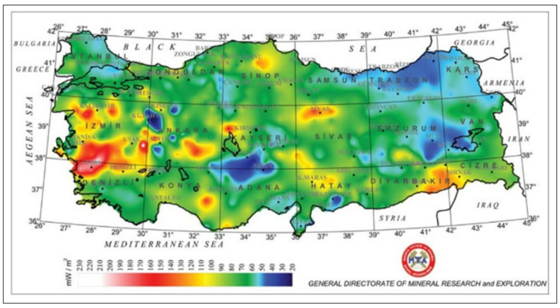

Figure 26: Heat Flow Map of Turkey [22].

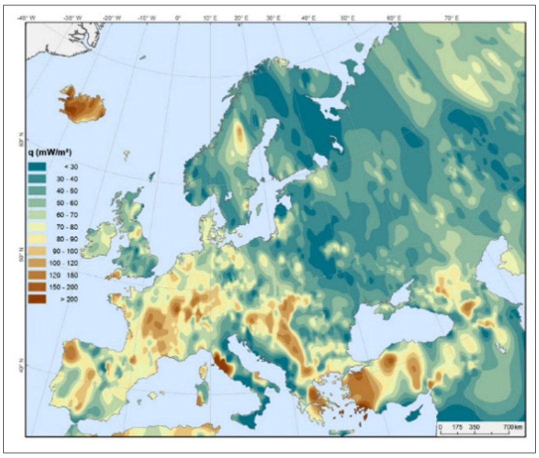

Figure 27: Surface Heat flow Map for Europe [23].

It is important to mark the earthquakes positions in Marmara Sea in April and August of 2025 (Figure 28, 29). Earthquakes are mostly in the boundaries of the sea.

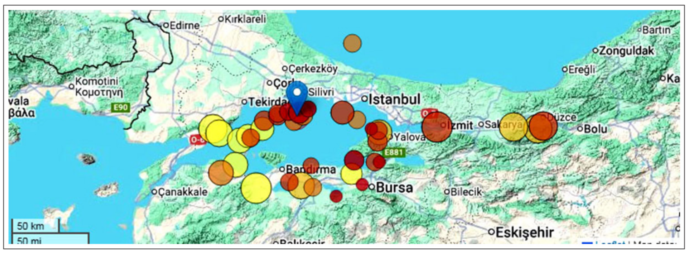

Figure 28: Map of Earlier Quakes in the Area of M 6.2 Earthquake, April 23, 2025. Oldest Quakes are Shown in Yellow, Most Recent in Red (USGS)

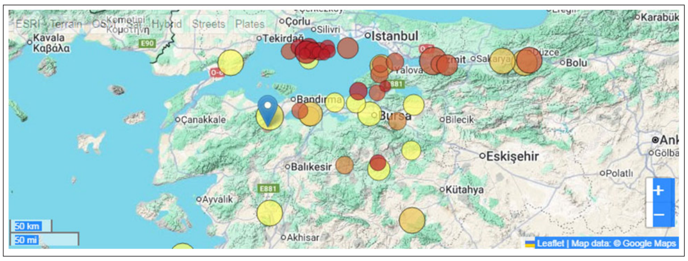

Figure 29: Map of Earlier Quakes in the Area of M 6.1 Earthquake, 10 August 2025, Sındırgı District of Balıkesir, Turkey, 8 km (5.0 mi) South-Southwest of Bigadiç. Oldest Quakes are Shown in Yellow, Most Recent in Red (USGS)

The Geodynamic Models of Natural Hazards Regions

Geological-geophysical and seismic tomography research give possibility to connect complicated geodynamics and stress-strain state of the region with upwelling of mantle flow from the core boundary (Figure 30, 31).

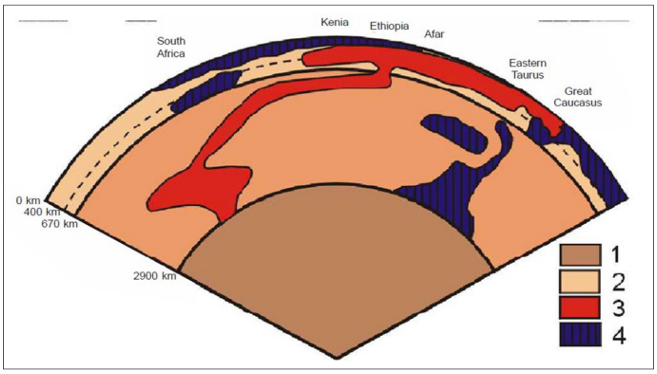

Figure 30: Schematic Seismotomographic Section Across the Mantle Along 120° Segment of the Great Circle Passing Through the Point with Coordinates 0° N and 35° E at Azimuth 10°, (1) the Earth Core; (2) Mantle; (3) Hot Low-Velocity Zones; (4) Cold High-Velocity Zones.
[24-26].

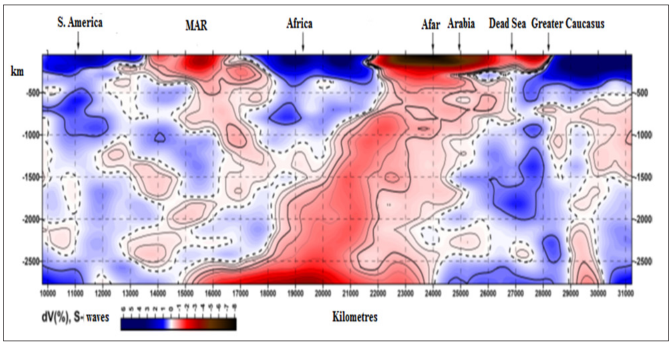

Figure 31: Section δV of NGRAND Seismic Tomographic Model Based on S-waves from Mantle Roof to its Base from western Coast of South America Across Atlantic Ocean, Africa, and Arabia to East European Platform. Zero isoline is shown by dotted line [27,28].

This upwelling of huge mantle flow is confirmed by magmatism and basalt volcanism (Figure 32-34).

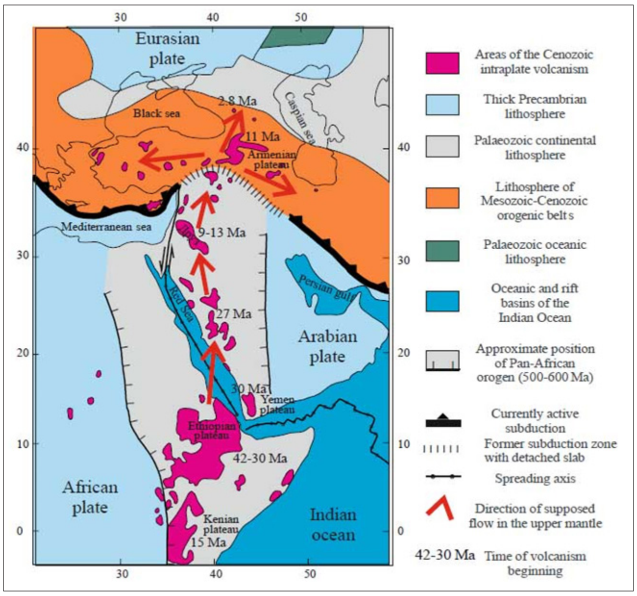

Figure 32: Tectonic Units and Distribution of Cenozoic Intraplate Plateau Basalt Volcanism and its Ages. Numbers Near Volcanic Plateaus Designate their age, Ma [24].

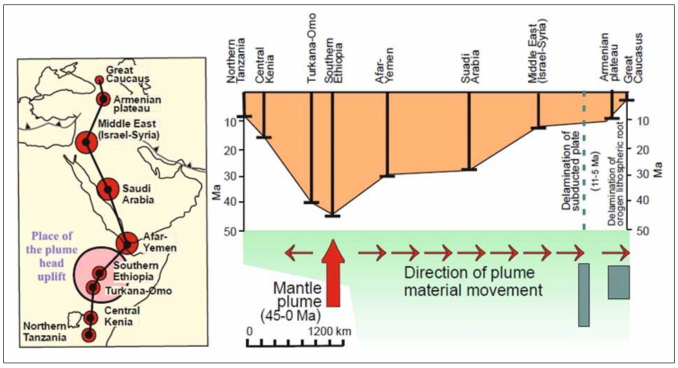

Figure 33: Age of Volcanic Activity Versus Distance Along the Hot Belt [24].

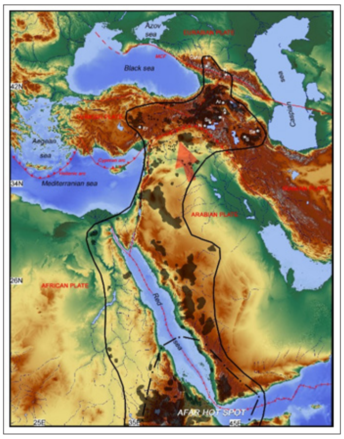

Figure 34: Distribution of the Modern Plume-Related Volcanism in the Afro-Arabian LIP (lithosphere plate) up to the Greater Caucasus. Black line-Contour of Projection of Proposed Mantle

Plume Head to the Surface. The Fields Painted by Black Represent the Areas of Young Volcanic Activity

The largest Quaternary volcanoes: A - Ararat, Ar - Aragats, CMW - Caucasian Mineral Waters, E - Elbrus, Er - Ercies, K - Kazbek, N - Nemrut, S - Savalan, Sa - Sahand, Su - Suphan, T – Tendürek [29,30]. Deep mantle flows extend north to the Caucasus region, where they divide into three branches: west to the Anatolian Plate, east to the Arabian Plate, and north to the Eurasian Plate and the Caucasus structure (Figure 35).

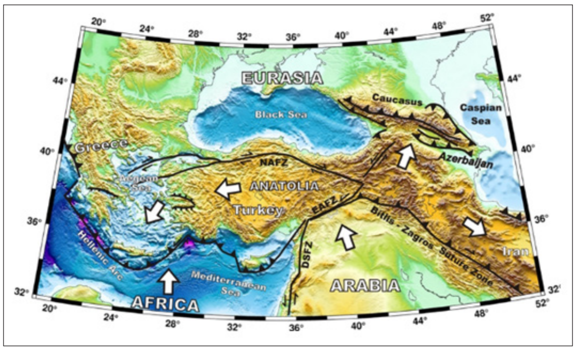

Figure 35: Geodynamics of the Caucasus-Anatolian-Arabian region (USGS)

The Zagros zone characterizes the collision of the Arabian, Anatolian and Eurasian plates (Figure 36-40).

Figure 36: Zagros Zone (USGS)

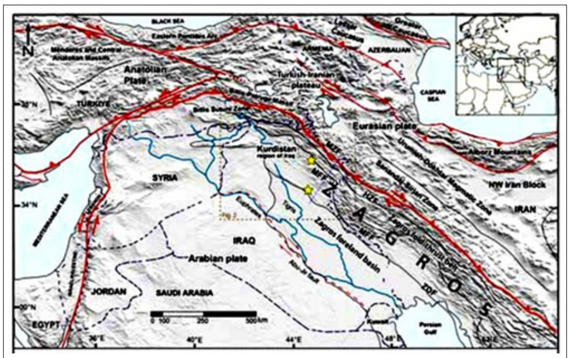

Figure 37: Tectonic Map of the Middle East in the Northwestern Segment of the Zagros Fold-Thrust Belt

MZF – Main Zagros Fault, HZF – High Zagros Fault, MFF – Mountain Front Flexure, ZDF – Zagros Deformation Front. Yellow stars – Representative location of subsidence curves. [31].

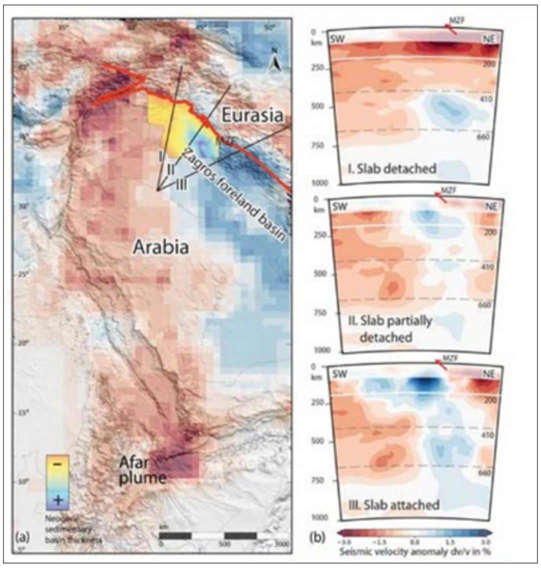

Figure 38: (a) Isopach Map of Neogene Deposits (~20–5 Ma) in the NW Zagros Foreland Basin
(b) Tomographic Cross Section Across Lines I, II, and III Across the NW Zagros Fold-Thrust Belt and Foreland Basin [31].

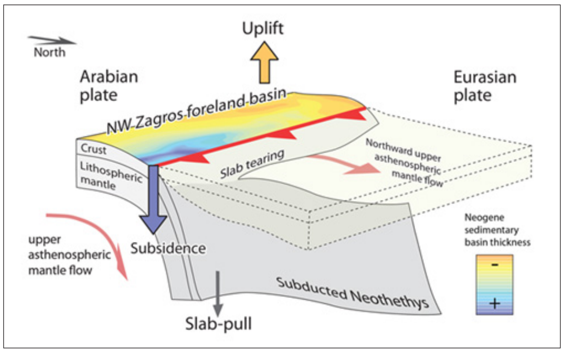

Figure 39: Geodynamic Scheme of the Zagros Zone [31].

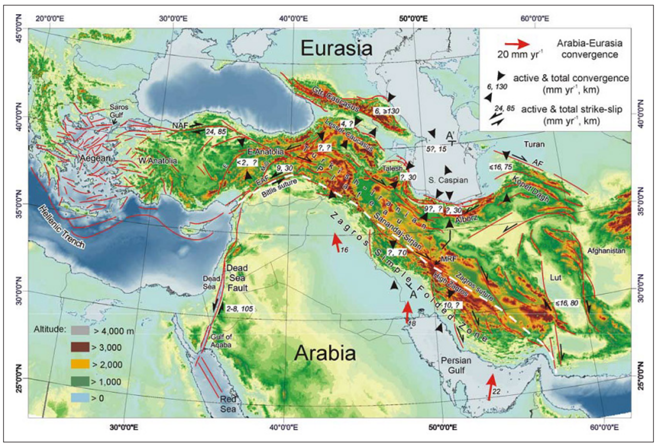

Figure 40: Topography, Structure, Current Deformation Rates and Finite Strain of the Arabia-Eurasia Collision

Abbreviations are as follows: AF- Ashgabat Fault, E- Ecemis¸ EAF, East Anatolian Fault M-O, Malatya-Ovacik Fault, MRF- Main Recent Fault, NAF- North Anatolian Fault Seismotomography of the Caucasus region shows mantle plumes and upwelling of the athenosphere (Figure 41) [32].

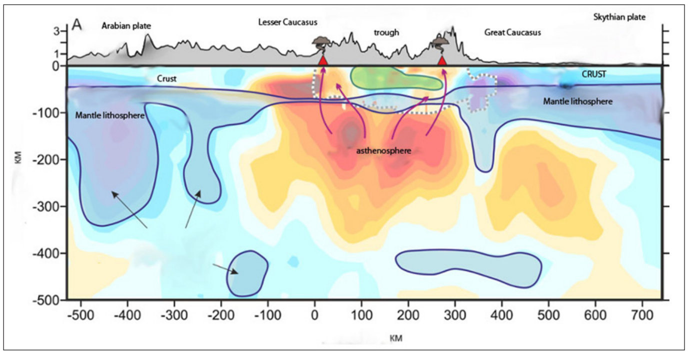

Figure 41: Seismotomographic Cross-Section of the Caucasus Region.
Lesser Caucasus, Great Caucasus, Caucasus Trough.
Red and yellow – asthenosphere, dark blue – mantle lithosphere, light blue – crust, green – higher density crust [33].

Results

Two possible mechanisms for reaching the ultimate strength of rocks at depth, leading to the formation of an earthquake foci, are possible. These are the activation of seismogenic faults due to horizontal movement of lithospheric plates and the vertical upwelling of material in the form of mantle diapirs due to gravitational instability. These mechanisms combine plate tectonics and plume tectonics. Both of these mechanisms are realized in the Sea of Marmara near Istanbul: activation of the North Anatolian Fault during earthquake foci advance from the east to the west and geothermal contrast in the lithosphere at the boundary of the rising mantle diapir off the coast in the Bosphorus region.

The propagation of earthquakes along the North Anatolian Fault and the East Anatolian Fault may be caused by deep mantle flow rising from the core beneath the Great African Rift, known on the Earth's surface as the Afar Plume. Deep mantle flows extend northward toward the Caucasus region, where they divide into three branches: westward toward the Anatolian Plate, eastward toward the Arabian Plate, and northward toward the Eurasian Plate and the Caucasus structure.

It can be assumed that strong earthquakes propagating along the North Anatolian Fault from east to west have passed the vicinity of Istanbul and are moving further west toward the Aegean Sea, as evidenced by the 2025 earthquake west of Istanbul. This suggests a decrease in the seismic risk for Istanbul in the near future in terms of horizontal movement along the fault.

The risk of a strong earthquake propagating along the North Anatolian Fault for Istanbul is reduced by the 2025 Marmara earthquake. At the same time, the risk of a possible earthquake similar to historical geothermal earthquakes remains high due to gravitational instability and the formation of an earthquake source near the depression boundaries. Such an earthquake, with a 250-year period (1509, 1766), could occur in the vicinity of Istanbul within the next few years.

As East Anatolian fault produced large earthquakes in 1789 (M 7.2), 1795 (M 7.0), 1872 (M 7.2), 1874 (M 7.1), 1875 (M 6.7), 1893 (M 7.1), 2020 (M 6.8), 2023 (M 7.8, M 7.7), it means that it is possible to link them in groups near 1790, 1880, 2020 with the frequency of groups (1790 – 1880 – 2020) near 100 years. But inside the groups there are 2-4 close in time large earthquakes. It could reflect matter rheology and lithosphere geodynamics of the region. It is necessary to investigate if 3 last large earthquakes of 2020 and 2023 (2) produced enough relaxation of material or not. As there were many aftershocks after 2023 earthquakes and they continue, maybe the next large earthquake there will be not so soon but in 100 years only. It is possible to forecast that if large earthquake in Earst Anatolian fault did not occur in 1-2 years after 2023, it will happen in 100 years only [34].

Conflict of Interest: the author declares no conflict of interest.

Acknowledgments
The article was prepared in response to a government assignment, research topic FMWM-2025-0004 "Development of methodological foundations for studying hazardous geological processes"; research topic № 125021902588-3 "Methodological foundations for assessing the state of the natural environment and the integral risk of hazardous processes of various natures in a mountainous region".

References

1. SE Güvercin, H Karabulut, AÖ Konca, U Doğan, S Ergintav (2022) Active seismotectonics of the East Anatolian Fault. Geophysical Journal International 230: 50-69.
2. Ross S. Stein, Aykut A. Barka, James H. Dieterich (1997) Progressive failure on the North Anatolian fault since 1939 by earthquake stress triggering, Geophysical Journal International 128: 594-604.
3. Marco Bohnhoff, Fatih Bulut, Georg Dresen, Peter E. Malin, Tuna Eken et al. (2013) An earthquake gap south of Istanbul. Nature Communications 4:1999.
4. Stein RS, Sevilgen V (2025) A magnitude 6.2 quake strikes the Marmara Fault at the site of large historic earthquakes near Istanbul. Temblor https://temblor.net/earthquake-insights/a-magnitude-6-2-quake-strikes-the-marmara-fault-at-site-of-large-historic-earthquakes-near-istanbul-16755/.
5. NN Ambraseys, JA Jackson (2000) Seismicity of the Sea of Marmara (Turkey) since 1500.Geophysical Journal International 141: F1-F6.
6. Barka A, Kadinsky-Cade K (1988) Strike-slip fault geometry in Turkey and its impact on earthquake activity. Tectonics 7: 663-684.
7. Taymaz T, Jackson J, McKenzie D (1991) Active tectonics of the north and central Aegean Sea. Geophys J Int 106: 433-490.
8. Okay AI, Demirbag E, Kurt H, Okay N, Kuscu I, (1999) An active, deep marine strike-slip basin along the North Anatolian Fault Turkey. Tectonics 18: 129-147.
9. Straub C, Kahle H G, Schindler C (1997) GPS and geologic estimates of the tectonic activity in the Marmara Sea region, NW Anatolia. J geo phys Res 102: 27587-27601.
10. S McClusky, S Balassanian, A Barka, C Demir, S Ergintav, et al. (2000) Global Positioning System constraints on plate kinematics and dynamics in the eastern Mediterranean and Caucasus. Journal of geophysical research 105: 5695-5719.
11. Garzón P, Bohnhoff M, Nurlu M (2020) Crustal thickness variation across the Sea of Marmara region, NW Turkey: A reflection of modern and ancient tectonic processes. Tectonics 39: e2019TC005986.
12. Uğur AKIN (2016) Investigation of the seismic velocity distribution and crustal structure of Turkey by means of gravity data. Bulletin of the Mineral Research and Exploration 153: 185-202.
13. Irina Artemieva, Rolf Meissner (2012) Crustal thickness controlled by plate tectonics: A review of crust–mantle interaction processes illustrated by European examples. Tectonophysics 530: 18-49.

14. Svalova VB (2019) Geothermy and seismicity of the Caucasus region and the inverse problem of geodynamics. Geology and Geophysics of the South of Russia 9: 77-93.
15. VB Svalova, VB Zaalishvili (2024) Deep geodynamics and seismicity of the Caucasus-Anatolian region. Geology and Geophysics of the South of Russia 14: 77-89.
16. VB Svalova, VB Zaalishvili (2024) Geodynamics and Geoecology. Moscow - Vladikavkaz: GPI VNC RAS 346 https://cgiras.ru/en.
17. Zabarinskaya L, Sergeyeva N, Rashidov V, Nisilevich M, Krylova T (2021) Structure and Dynamics of the Lithosphere for the Eurasia-Pacific Transition Zone. Heat-Mass Transfer and Geodynamics of the Lithosphere 411-428.
18. Leonardo Seeber, Christopher C Sorlien, Michael S Steckler, Marie-Helene Cormier (2010) Continental Transform Basins: Why Are They Asymmetric? Eos Transactions American Geophysical Union 91: 21-40.
19. Cecilia MG Mchugh, Leonardo Seeber, Marie-Helene Cormier, Matthew Hornbach (2014) Submarine Paleoseismology Along Populated Transform Boundaries: The Enriquillo-Plantain-Garden Fault, Canal du Sud, Haiti, and the North Anatolian Fault, Marmara Sea, Turkey. Oceanography 27:118-131.
20. Jean Schmittbuhl, Hayrullah Karabulut, O Lengliné, M Bouchon (2015) Seismicity distribution and locking depth along the Main Marmara Fault, Turkey. Geochemistry, Geophysics, Geosystems 17: 954-965.
21. G Göktürkler, M Salk, C Sari (2003) Numerical modeling of the conductive heat transfer in western Anatolia. Journal of the Balkan geophysical society 6: 1-15.
22. Bulletin of Mineral Research and Exploration. General Directorate of Mineral Research and Exploration, Turkey https://oaji.net/journal-detail.html?number=6459.
23. César R. Chamorro, José L García-Cuesta, María E Mondéjar, Alfonso Pérez-Madrazo et al. (2014) Enhanced geothermal systems in Europe: An estimation and comparison of the technical and sustainable potentials. Energy 65: 250-263.
24. Ershov AV, Nikishin AM (2004) Recent geodynamics of the Caucasus-Arabia-East Africa region. Geotectonics 38: 123-136.
25. Bijwaard H, Spakman W, Engdahl ER (1998) Closing the gap between regional and global travel time tomography. J Geophys Res 103: 30055-30078.
26. Zhou H (1996) A high-resolution P wave model for the top 1200 km of the mantle. J Geophys Res 101: 27791-27810.
27. Becker TW, Boschi LA (2002) Comparison of tomographic and geodynamic mantle models. Geochem Geophys Geosyst 3: 1-48.
28. Grand SP, van der Hilst RD, Widiyantoro S (1997) Global seismic tomography: A snapshot of convection in the Earth. GSA Today 7:1-7.
29. Sharkov EV, Lebedev VA, Rodnikov AG, Chugaev AV, Sergeeva NA, et al. (2012) Features of Caucasian segment of the Alpine-Himalayan convergence zone: geological, volcanological, Neotectonical, and geophysical data. Tectonics - Recent Advances 37-50.
30. Evgenii V Sharkov, Vladimir A Lebedev (2021) Caucasian-Arabian Segment of Alpine-Himalayan Convergence: an Example of Continental Collision above Mantle Plume. Heat-Mass Transfer and Geodynamics of the Lithosphere 381-390.
31. Koshnaw RI, Kley J, Schlunegger F (2024) The Miocene subsidence pattern of the NW Zagros foreland basin reflects the southeastward propagating tear of the Neotethys slab. Solid Earth 15: 1365-1383.
32. Allen M, Jackson J, Walker R (2004) Late Cenozoic reorganization of the Arabia-Eurasia collision and the comparison of short-therm and long-therm deformation rates. Tectonics 23: 1-17.
33. Koulakov I, Zabelina I, Amanatashvili I, Meskhia V (2012) Nature of orogenesis and volcanism in the Caucasus region based on results of regional tomography. Solid Earth 3: 327-337.
34. Zhao D (2001) Seismic structure and origin of hotspots and mantle plumes. Earth Planet Sci Let 192: 423-436.